changes concern mainly the g_x and g_y components, they are probably located close to the xy-plane of the O^- ion. The difference in the environment should be related probably to the presence or absence of charged nuclei with zero nuclear spin, i.e. most probably Ca^{2+} at z = 0.00 or 0.50.

The ENDOR spectra were recorded for several magnetic field settings within the EPR envelope, from $g = g_x$ to $g \approx 2.00$. A typical ENDOR spectrum of heated tooth enamel is shown in Fig.2. The ENDOR spectrum consists of four sets of peaks centered around the nuclear Zeeman frequencies of

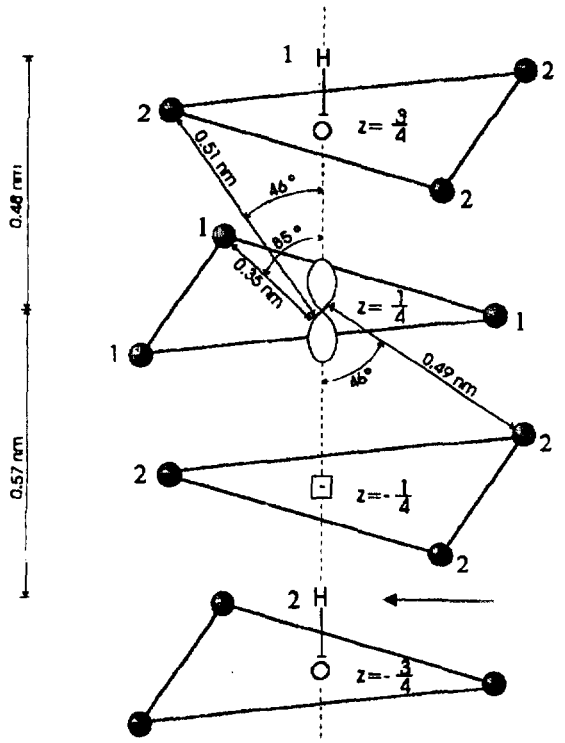

Fig.3. Model of O^- ion in heated tooth enamel hydroxyapatite as detected from the EPR and ENDOR results. The additional proton interaction, in comparison with the synthetic apatite, is indicated by the arrow.

^{23}Na, ^{31}P, ^{19}F and ^{1}H, respectively, in contradistinction to the synthetic apatite, where the interaction with ^{19}F is not visible. The ^{31}P and ^{1}H lines exhibit spectral resolution (three doublets for ^{31}P and two for ^{1}H) and these two resonances were analyzed using "orientation selection principle" [3, 4].

In our opinion, the ENDOR results support the model given by Moens et al. [1] wherein the O^- radical is located at an A site with the p_z orbital lobe oriented parallel to the hexagonal c axis. The model is shown in Fig.3.

The nearest-neighbouring phosphorus nuclei are distant of 0.35 nm and situated in the xy-plane of the O^- ion. The next-nearest-neighbouring phosphorus nuclei are situated in the mirror planes above and below the O^- radical position. They are at a distance of 0.5 nm and the angle between the c axis (p_z lobe) and the direction, connecting the unpaired electron and the phosphorus nuclei (θ_N), is 46°. The third doublet of ^{31}P corresponds with a nucleus located at a distance larger than 0.6 nm.

The nearest-neighbouring proton (interaction 1) belongs to the OH group located at the nearest occupied hydroxyl site and is pointing away from the O^- radical. This proton is 0.48 nm distant from the average position of the unpaired electron. On the other hand one of the nearest hydroxyl sites is vacant (see also [1]). The next-nearest-neighbouring proton, perhaps weakly visible in the synthetic apatite samples, originates from the hydroxyl group of z = -3/4. This nucleus is pointing towards the O^- radical and is at a distance of 0.57 nm. This proton is labelled 2 and indicated by an arrow in Fig.3.

All four resonances, as present in the ENDOR spectrum of the heated enamel powder, were examined by the EIEPR method. The EIEPR spectra of ^{31}P and ^{1}H show, that two radicals contribute to the total ENDOR spectra: the O^- ion radical and a radical, which has the following spin Hamiltonian parameters: $g_x = 2.003$, $g_y = 1.997$ and $g_z = 2.002$. A radical with these parameters is well known: it is obviously the CO_2^- radical. The latter radical probably causes mainly the large ^{1}H and ^{31}P matrix ENDOR lines. The EIEPR spectra of ^{19}F and ^{23}Na show evidently, that only the CO_2^- radical is responsible for ENDOR resonances. This could mean that probably fluor and sodium are located at the surface of the crystallites. The reason for the preferential position of F and Na close to the surface is not quite clear but could be related to the heating procedure.

References

[1]. Moens P., Callens F., Van Doorslaer S., Matthys P.: Phys. Rev., B 53, 5190-5197 (1996).

[2]. Sadło J., Callens F., Michalik J., Stachowicz W., Matthys P., Boesman E.: Calcif. Tissue Int. (1996), sent for publication.

[3]. Rist G., Hyde J.: J. Chem. Phys., 52, 4633-4643 (1970).

[4]. Moens P.D.W., Callens F.J., Matthys P.F., Verbeeck R.M.H.: J. Chem. Soc. Faraday Trans., 90(8), 2653-2662 (1994).

DAMAGE BUILDUP AND AMORPHIZATION IN ION - IMPLANTED $GaAs_{1-x}P_x$

S. Warchoł, J. Krynicki, H. Rzewuski, R. Groetzschel[1/]

[1/] FZR Forschungszentrum Rossendorf, Dresden, Germany

Ion implantation technique is widely used for doping and modifying semiconductor materials, providing important means of fabrication of a variety of devices for micro- and optoelectronic applications.

Depending on implantation conditions (ion mass, dose, dose rate, temperature) the damage produced may consist of various defect configurations, which for high ion doses create a heavily damaged or fully amorphous layer at the surface of a crystal.

Various models have been used to explain the nature of heavily damaged crystals and to propose the processes leading to amorphization.

Two presently accepted phenomenological models describe the crystalline-to-amorphous transition [1, 2] for III-V compounds as: a homogeneous or CED model (the crystal becomes unstable at some critical defect concentration taking place at Critical Energy Density deposited into the sample) or heterogeneous or Overlap Model (overlapping of the discrete amorphous zones directly created in the ion cascade).

Attempts to determine the crystal damage dose (CDD) of implanted ions and the critical energy density (CED) necessary for amorphous transition have usually been made.

Annealing properties and the crystal quality of the implanted layer depend very strongly on the kind and concentration of post-implantation defects [3].

It was shown by J.S. Williams and M.W. Austin [4] that under appropriate implantation conditions it is possible to regrowth amorphous layer of GaAs in a single-stage epitaxial process at temperatures as low as 370-420 K (compared to oven annealing above 900 K [5]).

On the other hand, the defect structures in a heavily damaged layer can evolve upon annealing into a more extended dislocation network, which usually lowers dopant activation. In such cases there is a need to avoid implantation conditions favouring the amorphization.

From this point of view the knowledge of what solid state properties dominate the amorphization processes and the subsequent recrystallization under given experimental conditions are of considerable interest.

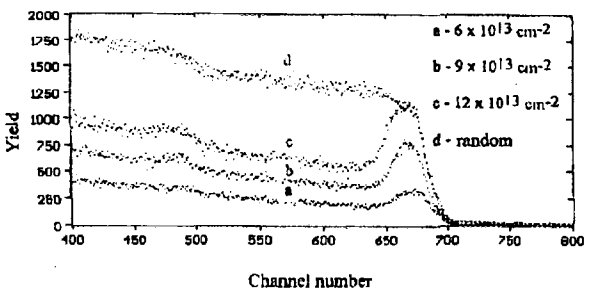

Fig.1. RBS spectra for $GaAs_{0.61}P_{0.39}$ implanted with As ions of 150 keV and for various fluences at 300 K.

Damage formation and amorphization processes in binary III-V compounds and some of ternary ones (e.g. AlGaAs) have been studied extensively.

However, only few papers have been devoted to $GaAs_{1-X}P_X$ [6, 7], a wide gap semiconductor (E_g = 1.4-2.2 eV depending on relative composition - x), being a promising ternary compound for electronic and optonic devices (FET, HEMT, HBT, LED, solar cells, heterojunction lasers).

In this paper we present results on the damage formation and amorphization of $GaAs_{1-X}P_X$ implanted with As^+ and P^+ ions under various experimental conditions.

The CDD and CED for amorphization have been evaluated providing the data for establishing the sensitivity of those compounds for damage and amorphous transition.

RBS-c spectroscopy of 1.7 MeV He^+ ions was used to measure the residual, postimplantation damage.

Monocrystalline $GaAs_{1-X}P_X$ epilayers 0.5 μm thick, grown by liquid phase epitaxy on <100> GaAs (Te) substrate were used. The samples having x = 0.15, 0.39 and 0.65 content of P have been investigated. For comparison, binary samples GaAs and GaP were also measured.

Table 1. Implantation conditions for $GaAs_{1-X}P_X$ layers (x = 0, 0.15, 0.39, 0.65, 1.0).

Ions	P^+		As^+	
Temperature [K]	120	300	120	300
Ion energy [keV]	100		150	
Ion dose [10^{13} cm^{-2}]	2	3	1	1
	4	6	2	1.5
	9	9	3.5	2
	12	12	5	2.5
				3.5
				5

The implantation conditions are presented in Table 1. By way of example, random and aligned RBS spectra of $GaAs_{0.61}P_{0.39}$ implanted with As and P ions were given in Figs. 1 and 2. Similar

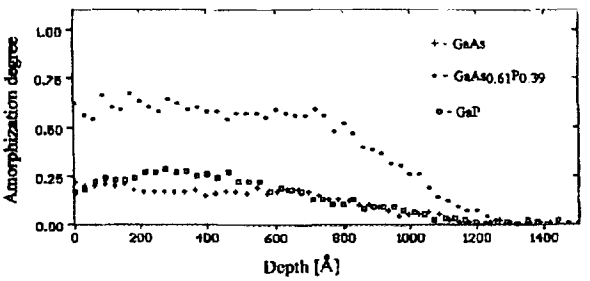

Fig.3. Damage depth distribution for 2 x 10^{13} cm^{-2}, 150 keV As ion implantation of $GaAs_{1-X}P_X$ at 300 K.

spectra were measured for other experimental conditions shown in Table 1. They were used to

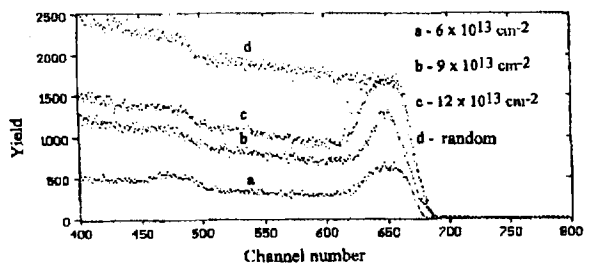

Fig.2. RBS spectra for $GaAs_{0.61}P_{0.39}$ implanted with P ions of 100 keV and for various fluences at 300 K.

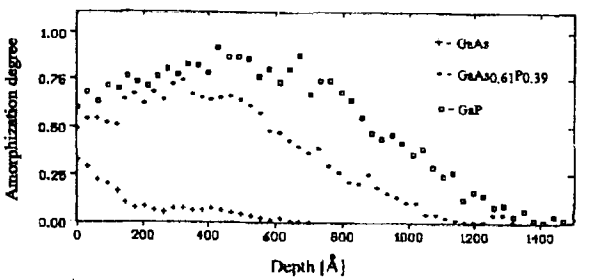

Fig.4. Damage depth distribution for 9 x 10^{13} cm^{-2}, 100 keV P ion implantation of $GaAs_{1-X}P_X$ at 300 K.

Table 2. Critical damage dose (CDD) and Critical Energy Density (CED) for $GaAs_{1-X}P_X$ implanted with As and P ions.

	CDD [x 10^{13} cm^{-2}]				CED [x 10^{20} keV cm^{-3}]			
	As - 150 keV		P - 100 keV		As - 150 keV		P- 100 keV	
	120 K	300 K	120 K	300 K	120 K	300 K	120 K	300 K
GaAs	3.2	8	10.7	36	1.5	3.75	4.5	15.2
$GaAs_{0.85}P_{0.15}$	2.4	3.5	10.7	26.7	1.1	1.6	4.4	10.9
$GaAs_{0.61}P_{0.39}$	2.5	3.5	9	12.4	1.05	1.47	3.4	4.7
$GaAs_{0.35}P_{0.65}$	3.0	3.5	6.2	9	1.12	1.3	2.0	3.0
GaP	4.2	8	7.6	10.5	1.28	2.4	2.1	2.9

calculate the depth damage distributions (damage profile) using a known formula [8] and a computer program TRIM'95 (Figs. 3 and 4).

As can be seen from these spectra, the highest amorphization level, i.e. the highest sensitivity to the damage, occurs for ternary samples implanted with As ("heavy ion") and for a binary GaP sample implanted with P ("light ion").

Table 2 presents the CDD and CED values for $GaAs_{1-X}P_X$ for P and As ion implantation at 120 and 300 K.

The CDD is an extrapolated value of ion dose for 95% of the total amorphization measured at R_p.

The CED represents the energy deposited in a crystal to create full amorphization of a layer, calculated with the use of computer program TRIM'95.

These data vs. the compound composition x are presented in Fig.5.

As could be expected from the previous results [8], a considerable nonlinearity of amorphization degree vs. x occurred for both CDD and CED values.

Ternary compounds appeared more sensitive to amorphization with respect to the P content.

The minimum of damage level occurs for a definite composition x (with the exception of CED, P - implantation, 100 keV, 300 K) for both low and high temperature of implantation.

The CED results for binary samples GaAs and GaP are higher for GaAs and lower for GaP, with accordance with the paper by Jones and Santana [9].

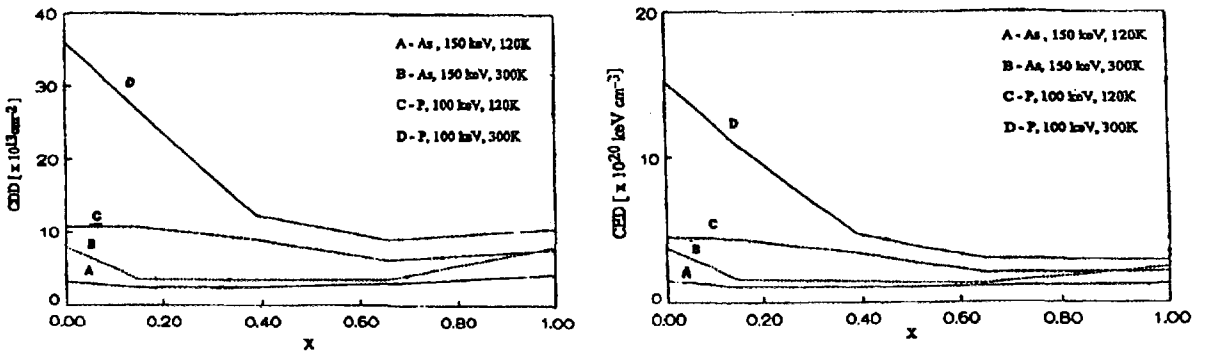

Fig.5. Critical damage dose and critical energy density for amorphization as a function of sample composition x after As and P ion implantation at 120 and 300 K.

Further works on the model describing the crystalline-to-amorphous transition for As and P ion implantation in the investigated ternary compounds $GaAs_{1-X}P_X$ will be carried on.

References

[1]. Chadderton L., Eisen F.H.: Proc. 1st Int. Conf. on Ion Implantation. Gordon and Breach, New York 1971, p. 445.

[2]. Gibbons J.F.: Proc. IEEE, 56, 295 (1968).

[3]. Wendler E., Muller P., Bachmann T., Wesh W.: Nucl. Instr. Meth. Phys. Res. B, 80/81, 711 (1993).

[4]. Williams J.S., Austin M.W.: Nucl. Instr. Meth., 168, 307 (1980).

[5]. Grimaldi M.G., Paine B.M., Maenpaa M., Nicolet M.A., Sadana D.K.: Appl. Phys. Lett., 39, (1), 70 (1981).

[6]. Mooney P.M.: Appl. Phys. Rev., J. Appl. Phys., 67, R1 (1990).

[7]. Krynicki J., Warchoł S., Rzewuski H., Groetzschel R.: Acta Phys. Pol., A87, 249 (1995).

[8]. Chu W.K., Mayer J.W., Nicolet M.A.: Backscattering Spectroscopy. Academic Press, New York 1978.

[9]. Jones K.S., Santana C.J.: J. Mater. R(

DOSIMETRIC RESPONSE OF MICROCRYSTALLINE L-α-ALANINE AND STANDARD BONE POWDER TO HIGH-LET RADIATIONS

Z. Stuglik, J. Sadło

Stable EPR-signals induced in bone and other materials have been successfully used for nuclear accidents retrospective dosimetry [1] and for the estimation of doses accumulated by inhabitants of nuclear contaminated areas [2]. In such kind non-controlled conditions the doses accumulated by human beings arise from various kind of low- and high-LET radiations. Thus, the accuracy of dosi-